Hindawi

Research Article

A Miniaturized Dual-Band Short-Ended ZOR Antenna with Backed Ground Plane for Improved Bandwidth and Radiation Efficiency

Rajkishor Kumar [iD],[1] **Avinash Chandra** [iD],[1] **Sreenath Reddy Thummaluru** [iD],[2] **Mohammad Monirujjaman Khan** [iD],[3] **and Raghvendra Kumar Chaudhary** [iD][4]

[1]*School of Electronics Engineering, Vellore Institute of Technology, Vellore, Tamil Nadu 632014, India*
[2]*Department of Electronics and Communication Engineering,*
  Indian Institute of Information Technology Design and Manufacturing (IIITDM), Kancheepuram, Chennai 600127, India
[3]*Department of Electrical and Computer Engineering, North South University, Bashundhara, Dhaka-1229, Bangladesh*
[4]*Department of Electrical Engineering, Indian Institute of Technology Kanpur, Kanpur 208016, India*

Correspondence should be addressed to Mohammad Monirujjaman Khan; khandrmohammadmonirujjaman@gmail.com

This paper presents a miniaturized planar dual-band short-ended metamaterial antenna with the backed ground plane to improve antenna bandwidths and radiation characteristics. The proposed dual-band metamaterial (MTM) antenna has been made up of the composite right- or left-handed transmission line (CRLH-TL) concept. Here, the backed ground plane has been employed to generate an extra coupling capacitance (C_C), which shifts the ZOR frequency in the lower band while also improving ZOR matching and increasing the impedance bandwidth of the higher-order mode. In this proposed MTM antenna, interdigital capacitance (IDC) has been used in place of a simple series gap, which shifts the higher-order impedance bandwidth into a lower frequency band for second-band Wi-MAX applications (3.3–3.7 GHz). The proposed antenna offers a short-ended MTM, and hence the ZOR frequency is controlled by a series of LC lumped parameters. The proposed antenna offers dual-band behavior with measured −10 dB impedance bandwidths of 5.55% and 41.57% at centered frequencies of 2.70 GHz and 4.33 GHz, respectively. The overall electrical size of the designed antenna is $0.225\lambda_0 \times 0.144\lambda_0 \times 0.0144\lambda_0$ at ZOR ($f_0 = 2.70$ GHz), where λ_0 is the free space wavelength; therefore, it is applicable for different Wi-MAX application bands (2.5–2.7 GHz/3.3–3.8 GHz). Furthermore, the proposed dual-band MTM antenna provides compactness, low loss, stable gain, and radiation efficiency, and also offers omnidirectional radiation patterns in the *E*-plane and dipolar type radiation patterns in the *H*-plane, respectively.

1. Introduction

In a metamaterial antenna, the zeroth-order resonance is a special property derived by plotting the dispersion characteristics of composite right- or left-handed transmission lines (CRLH-TL). In the zeroth-order resonant (ZOR) mode, the physical size of the antenna is independent of the resonant frequency [1–8]. Since metamaterial (MTM) is an artificial structure, it has some unnatural properties, such as group and phase velocities being in opposite directions and a nonlinear progressive phase [9, 10]. Several works have been performed based on the ZOR property to miniaturize the size of the antenna, despite the fact that it has a narrow bandwidth, negative gain, and poor radiation efficiency [11, 12]. In recent years, numerous methods have been introduced to improve the impedance bandwidth, gain, and radiation efficiency of metamaterial antenna [13]. Short-ended MTM antenna offers designed flexibility for the antenna community to control ZOR frequency by varying series parameters [14]. Due to the recent requirement of different wireless communication bands in one system, dual or multiband antennas are more demanding to fulfill these

requirements. The advantages of dual or multiband antennas are that they reduce the number of antennas and space usage and also overcome interference between other frequency bands [15–17]. Many dual-band compact ZOR antennas have been reported in recent years, but these dual-band MTM antennas have suffered from impedance bandwidth peak gain and radiation efficiency [18–22]. So, there are very big challenges for the antenna community to design such a type of dual-band MTM antenna to remove all these drawbacks.

In this context, a compact short-ended CPW-fed ZOR antenna for dual-band applications has been presented. The proposed dual-band MTM antenna improved the ZOR and other higher-order mode impedance bandwidths and radiation efficiencies without affecting its compactness. The designed antenna is basically based on short-ended termination; thus, ZOR frequency depends on LC series parameters and can be controlled by varying series elements of the antenna. Here, an interdigital capacitor is provided, shifting the second resonating frequency towards the lower band. In addition, the backed ground plane improves matching, shifting the frequency on the lower side, and creating wideband nature. The advantages of the proposed antenna are its compactness, low loss, CPW feeding, via-less design, easy fabrication process, low cost, realization of series parameters, and good radiation capacity.

2. Antenna Design Techniques

2.1. Composite Left- and Right-Handed Transmission Line (CRLH-TL) Theory. Figure 1 shows an equivalent circuit diagram of the proposed dual-band MTM antenna. It consists of left-handed shunt inductance L_L, right-handed series inductance L_R, left-handed series capacitance C_L, and right-handed shunt capacitance C_R. As per the CRLH-TL theorem, the resonance frequencies have been found using these four CRLH-TL parameters (L_L, L_R, C_L, and C_R), and they are independent of the size of the antenna.

From the Bloch and Floquet theory, the dispersion relation is determined for the unit cells of periodic structures, and it is reported in [9, 10].

$$\beta_{\text{CRLHTL}}(\omega) = \frac{1}{p}\cos^{-1}\left[1 + \frac{Z_{\text{CRHL}}(\omega) \times Y_{\text{CRLH}}(\omega)}{2}\right], \quad (1)$$

where

$$Z_{\text{CRLH}}(\omega) = j\left(\omega L_R - \frac{1}{\omega C_L}\right),$$

$$Y_{\text{CRLH}}(\omega) = j\left(\omega C_R - \frac{1}{\omega L_L}\right) \text{Without backed ground plane}, \quad (2)$$

$$Y_{\text{CRLH}}(\omega) = j\left(\omega C_R + \omega C_c - \frac{1}{\omega L_L}\right) \text{With backed ground plane}.$$

Here, the phase constant (β) is related to the Bloch wave, and p shows the unit cell length of the proposed dual-band MTM antenna.

The resonance frequency of the designed CRLH-TL based on a dual-band MTM has been found using the given equation

$$\beta_n p = \frac{n\pi p}{l} = \frac{n\pi}{N} \ (n = 0, 1, 2, 3, 4, \ldots\ldots\ldots\ldots, (N-1), \quad (3)$$

where l (=Np), n, and N are the length of the resonator, the resonance modes, and the unit cell number.

The designed dual-band MTM antenna is based on short-ended boundary conditions; therefore, the input impedance (Z_{in}) is found from one side of the resonator towards the other side, whereas the load impedance is zero ($Z_L = 0$). So, the input impedance (Z_{in}) is obtained by [9]

$$Z_{\text{in}}^{\text{short}} = -jZ_0 \times \tan(\beta l) \sim jZ_0 \times \beta l = j\sqrt{Z'_{\text{CRLH}}/Y'_{\text{CRLH}}}\left(\frac{\sqrt{Z'_{\text{CRLH}}Y'_{\text{CRLH}}}}{j}\right)l = Z'_{\text{CRLH}} \times l = Z \times Np, \quad (4)$$

where Z_0 is the characteristic of CRLH-TL, Z'_{CRLH} and Y'_{CRLH} are the series impedance and shunt admittance per unit periodic length.

When $n = 0$ (from (3)), the propagation constant $\beta = 0$ shows the ZOR mode, and the resonance frequency is obtained by
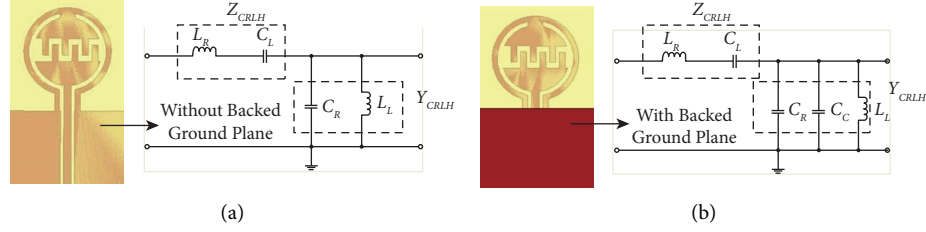
FIGURE 1: Equivalent circuit diagram (a) without backed ground plane, and (b) with backed ground plane of the proposed dual-band MTM antenna.

$$\omega_{\text{se}} = \omega_{\text{ZOR}} = \frac{1}{\sqrt{L_R C_L}}. \tag{5}$$

From (5), the ZOR frequency has been contained by variation of series capacitance (C_L) and inductance (L_R) of the proposed dual-band MTM.

2.2. Antenna Configuration. The configuration of the proposed dual-band MTM antenna is shown in Figure 2. The proposed MTM antenna has been fabricated on an FR4 glass-epoxy substrate ($\varepsilon_r = 4.4$, $\tan\delta = 0.02$) with a compactness of 1.6 mm.

It consists of a circular patch having an interdigital capacitor, a CPW ground plane, and a partially backed ground plane. The designed MTM antenna is fed by a 50 Ω microstrip line. The interdigital capacitance forms a series capacitor (C_L), while the small stripline acts as a shunt inductor (L_L), which verifies the composite right- or left-handed transmission line-based MTM. C_C is the coupling capacitance between the CPW feed and the partially backed ground plane, whereas C_R is the shunt capacitance obtained between the upper ground plane and the CPW feed. The series inductance (L_R) is realized by a signal patch. The overall electrical size of a designed dual-band MTM antenna is $0.225\lambda_0 \times 0.144\lambda_0 \times 0.0144\lambda_0$ at ZOR ($f_0 = 2.70$ GHz), where λ_0 is the free space wavelength.

2.3. Validation of ZOR Mode. To verify the short-ended condition of ZOR frequency, parametric analysis has been done based on the series element, i.e., L_R. Figure 3 shows the input reflection coefficient with different values of patch width called series inductor (L_R) with respect to frequency. It is found that ZOR frequency decreases towards the lower frequency band when patch width (W_F) increases, which confirms the behavior of ZOR mode. There is another way to verify the ZOR conditions of the proposed antenna by plotting the electric field at ZOR frequency. It is clearly observed from Figure 4 that the distributions of the electric field are showing in phase at 2.72 GHz. Therefore, it verified the ZOR condition occurred at a 2.72 GHz resonance frequency.

2.4. Effect of Backed Ground Plane. In this subsection, the effect of with and without backed ground plane on the input reflection coefficient has been demonstrated. It is observed from Figure 5 that, due to the backed ground plane, one more coupling capacitance (C_C) is introduced to shift the ZOR frequency from 3.3 to 2.72 GHz and also improve the higher-order impedance bandwidth of the designed antenna. This coupling capacitance helps to miniaturize the size of the antenna as well as the backed ground plane coupled with the radiator to improve the matching and enhanced impedance bandwidth.

2.5. Effect of Series Gap and Interdigital Capacitance. Here, the effect of the series gap and interdigital capacitance on the reflection coefficient has been studied, as shown in Figure 6. The spiral-shaped is nothing but interdigital capacitance, which provides more capacitive values compared with the inductive values in order to get good performance at the lower band of the proposed antenna structure. It is clearly observed from Figure 6 that the interdigital capacitance provides a better response compared to series gap capacitance and shifts the impedance bandwidth frequency to the lower side.

3. Simulated and Measured Results

A prototype antenna has been fabricated to verify the measured and simulated near- and far-field results, as shown in Figure 7. The Keysight programmable network analyzer (N5221A) has been used to measure near-field results, i.e., the input reflection coefficient. The simulated dual-band MTM antenna offers −10 dB input impedance bandwidth of 5.14% (2.65–2.79 GHz) and 30.37% (3.63–4.93 GHz) for the first and second bands, respectively, whereas the measured −10 dB input impedance bandwidth ($S_{11} < -10$ dB) offers 5.55% (2.63–2.78 GHz) and 41.57% (3.43–5.23 GHz) for the first and second band, respectively, as shown in Figure 8. The simulated and measured resonant frequency of ZOR is found to be 2.72 GHz and 2.70 GHz, respectively, and also higher-order impedance bandwidth increases. This happens due to imperfections in antenna fabrication and tolerance in soldering.

Figure 9 illustrates the normalized radiation patterns of the proposed antenna in the *xz*- and *yz*-plane at 2.72 GHz and 4.58 GHz, respectively. It is observed that at ZOR frequency (2.72 GHz) and 4.58 GHz, the proposed antenna shows an omnidirectional radiation pattern in the *xz*-plane. At frequencies 2.72 GHz and 4.58 GHz, it shows a dipolar type radiation pattern in *yz*-plane. The difference between copolarization and cross-polarization levels in the *xz*-plane is −46.53 dB at 2.72 GHz and −40.03 dB at 4.58 GHz.
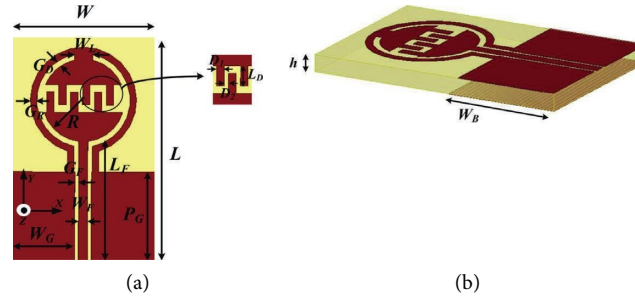
FIGURE 2: Geometry of proposed dual-band metamaterial antenna ($L = 25$, $W = 16$, $P_G = 10$, $W_G = 7.1$, $W_F = 1$, $G_F = 0.4$, $L_F = 13.5$, $R = 4.5$, $G_R = 0.7$, $G_D = 0.6$, $W_L = 2$, $D_1 = 0.8$, $D_2 = 0.5$, $L_D = 2.2$, $W_B = 11$, $h = 1.6$: all dimensions are in mm).
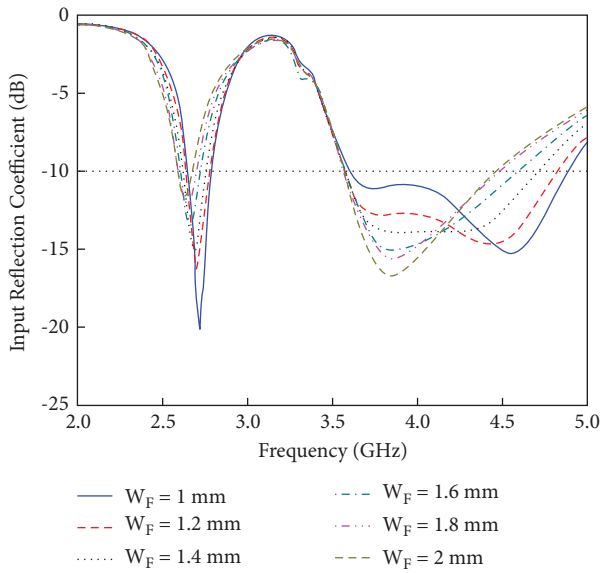

FIGURE 3: Simulated reflection coefficient of the proposed dual-band MTM antenna by varying W_{F3}.
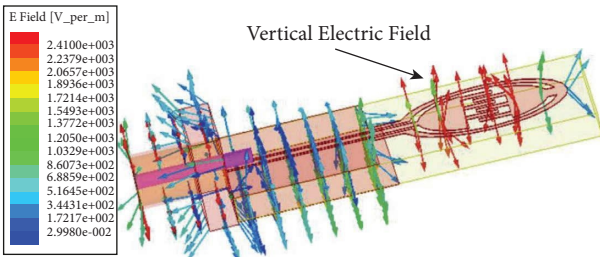

FIGURE 4: Electric field distribution to confirm the ZOR mode at 2.72 GHz.

The maximum gain of the proposed dual-band MTM antenna is 0.72 dBi for the first band and 2.0 dBi for the second band, respectively, whereas it shows a measured maximum peak gain of 0.59 dBi for the first band and 2.10 dBi for the second band, respectively [23], as shown in Figure 10(a). The designed dual-band MTM antenna shows an average radiation efficiency of 71.52% for the first band
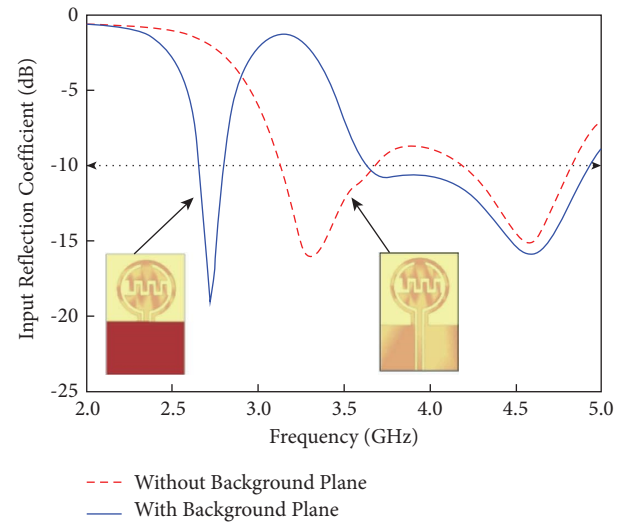

FIGURE 5: Input reflection coefficient of proposed dual-band MTM with and without backed ground plane.
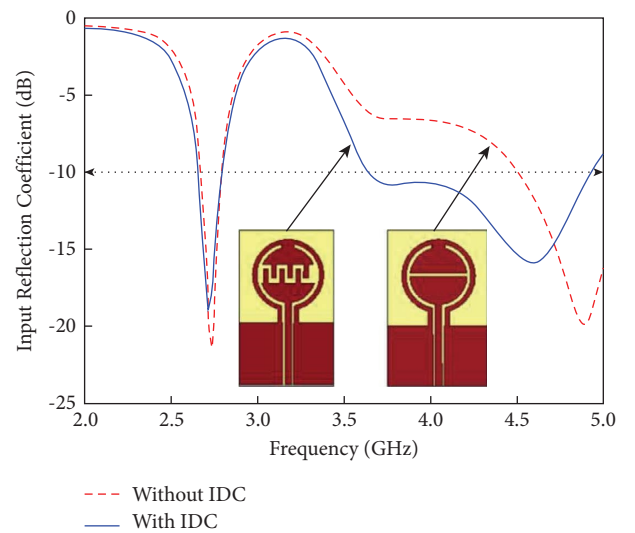

FIGURE 6: Input reflection coefficient of proposed dual-band MTM with and without IDC.
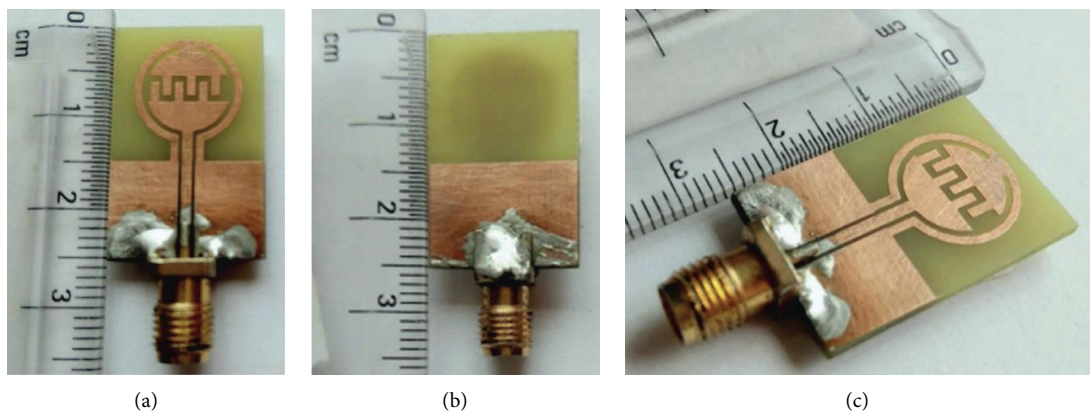
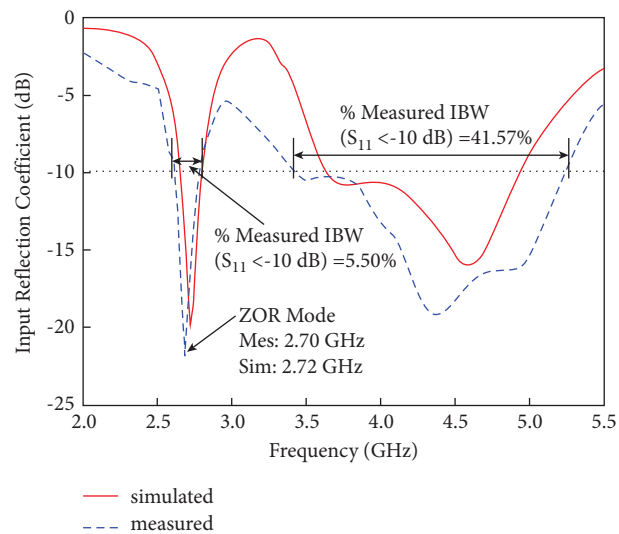FIGURE 7: Photograph of proposed dual-band MTM antenna: (a) top view, (b) ground plane, and (c) 3D view.

FIGURE 8: Simulated and measured input reflection coefficients of the proposed dual-band MTM antenna.
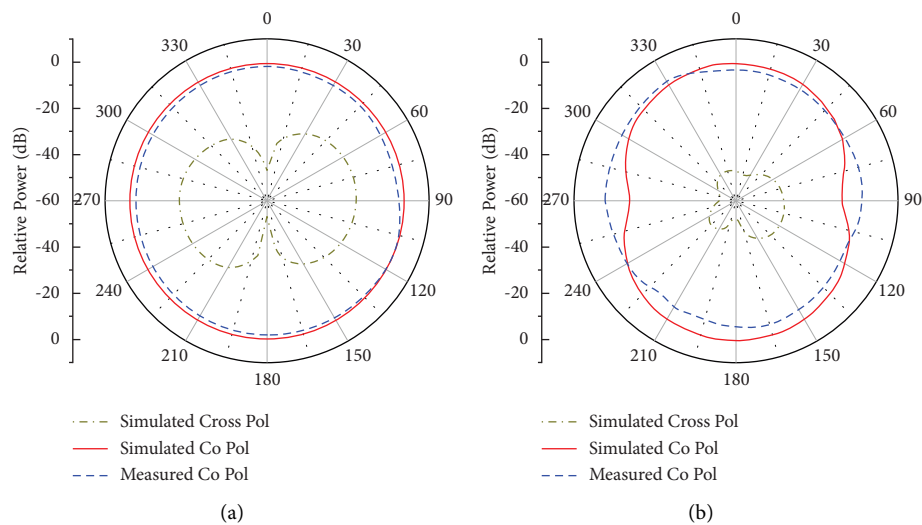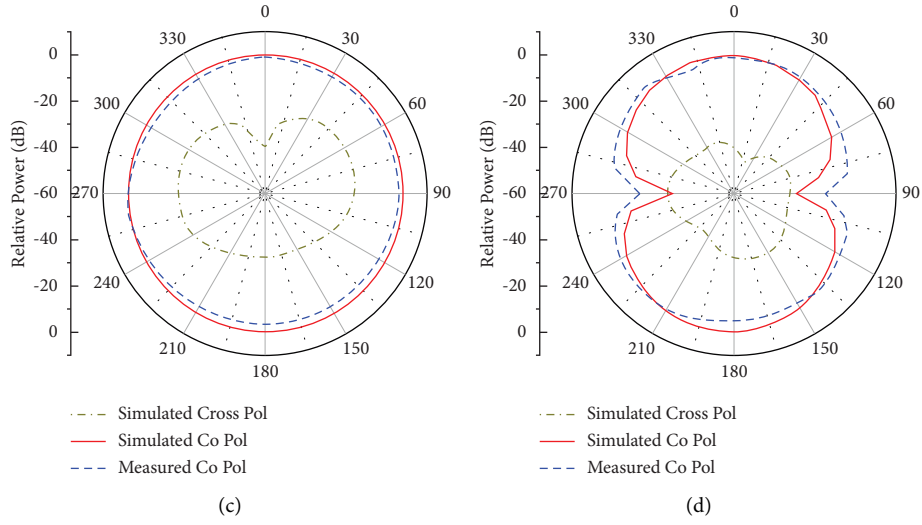

FIGURE 9: Continued.

(c)

(d)

FIGURE 9: Normalized radiation patterns: (a) *xz*-plane, 2.72 GHz; (b) *yz*-plane, 2.72 GHz; (c) *xz*-plane, 4.58 GHz; (d) *yz*-plane, 4.58 GHz of proposed dual-band MTM antenna.
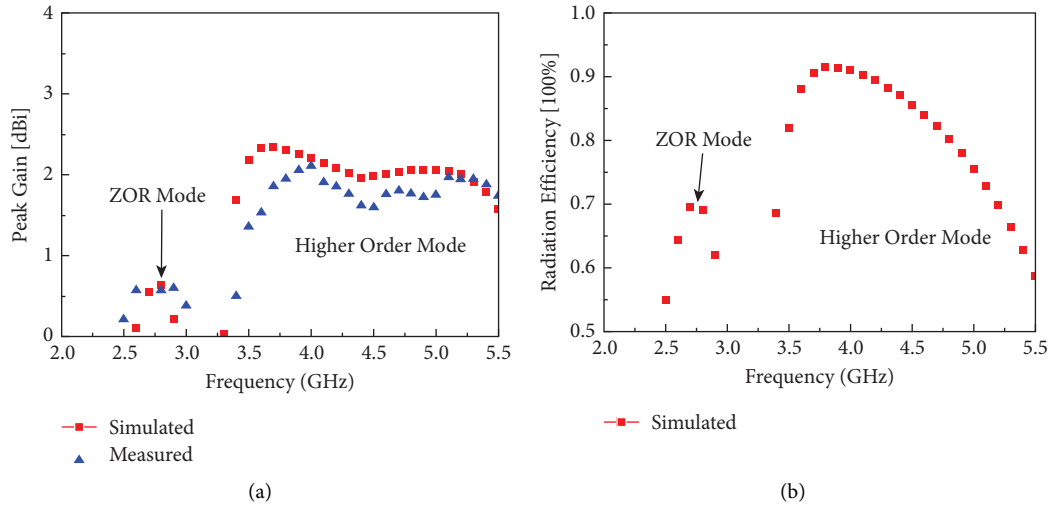

(a)

(b)

FIGURE 10: Far-field results of proposed dual-band MTM antenna in the broadside direction. (a) Simulated and measured gain; (b) radiation efficiency.

TABLE 1: Comparison of dual-band MTM antennas with recently published work.

Ref.	Antenna size	Resonance frequency (GHz)	Via process	−10 dB impedance bandwidth (%)	Gain (dBi)	Radiation efficiency (%)
[13]	$0.27\lambda_0 \times 0.23\lambda_0$	2.6/3.6	Not needed	2.29/28.57	0.53/1.98	NA[#]/NA[#]
[16]	$0.33\lambda_0 \times 0.098\lambda_0$	2.45/3.37	Not needed	8.16/23.74	0.3/1.1	68/77.3
[24]	$1.05\lambda_0 \times 1.05\lambda_0$	6.6/10.9	Needed	3.03/5.04	7.29/2.97	NA[#]/NA[#]
[25]	$1.27\lambda_0 \times 1.27\lambda_0$	1.73/5.36	Not needed	17.34/11.75	8.23/8.30	NA[#]/NA[#]
[26]	$0.021\lambda_0 \times 0.018\lambda_0$	0.91/2.45	Needed	17.8/35.8	−17.1/−9.81	NA[#]/NA[#]
[27]	$0.35\lambda_0 \times 0.45\lambda_0$	2.58/5.41	Not needed	20.6/15.7	3.5/3.53	NA[#]/NA[#]
PW*	$0.22\lambda_0 \times 0.14\lambda_0$	2.72/4.58	Not needed	5.50/41.57	0.72/2.0	71.52/84.02

NA[#] = not available, PW* = proposed work.

and 84.02% for the second band, as shown in Figure 10(b). Table 1 shows the comparison among dual-band MTM antennas with recently published work. It is observed that the advantages of the proposed dual-band MTM antenna are an overall improvement in impedance bandwidth, a high level of miniaturization, and via-less design.

4. Conclusion

A miniaturized CPW-fed dual-band short-ended ZOR-based antenna with the backed ground plane is investigated. The proposed antenna is short-ended, so the ZOR mode is dependent upon the series LC parameters of the proposed MTM antenna. The designed antenna consists of the backed ground plane to introduce extra capacitance, which is used to shift ZOR frequency towards a lower frequency band and miniaturize the size of the antenna. Here, instead of a series gap, an interdigital capacitance is used in the proposed antenna to lower the higher-order impedance bandwidth. The designed antenna offers dual-band behavior with measured −10 dB impedance bandwidths of 5.55% (centered at 2.70 GHz) and 41.57% (centered at 4.33 GHz) for the first and second bands, respectively. The proposed antenna shows a measured maximum peak gain of 0.59 dBi for the first band and 2.10 dBi for the second band, respectively, whereas it shows an averaged simulated radiation efficiency of 71.52% and 84.02% for the first and second bands, respectively. Furthermore, the proposed MTM offers a high level of compactness and an omnidirectional and dipolar type radiation pattern, which is suitable for Wi-MAX band applications.

Data Availability

The data that support the findings of this study are available from the corresponding author upon reasonable request.

Conflicts of Interest

The authors declare that there are no conflicts of interest regarding the publication of this paper.

References

[1] J. Fu and O. H. Raheem, "A novel IMSL tunable phase shifter for HMSIW-LWA-fed rectangular patches based on nematic liquid crystal," *Applied Physics A*, vol. 123, no. 7, pp. 493–498, 2017.

[2] A. Kumar and S. Imaculate Rosaline, "Hybrid half-mode SIW cavity-backed diplex antenna for on-body transceiver applications," *Applied Physics A*, vol. 127, no. 11, pp. 834–837, 2021.

[3] D. Chaturvedi, A. A. Althuwayb, and A. Kumar, "Bandwidth enhancement of a planar SIW cavity-backed slot antenna using slot and metallic-shorting via," *Applied Physics A*, vol. 128, no. 3, pp. 193–2022, 2022.

[4] L. Fagiolari, E. Varaia, N. Mariotti, M. Bonomo, C. Barolo, and F. Bella, "Poly (3, 4-ethylenedioxythiophene) in dye-sensitized solar cells: toward solid-state and platinum-free photovoltaics," *Advanced Sustainable Systems*, vol. 5, no. 11, Article ID 2100025, 2021.

[5] A. A. Althuwayb, "SIW cavity-backed slot antenna with monopole-like radiation for vehicular communications," *Applied Physics A: Materials Science & Processing*, vol. 202, 2022.

[6] A. Sanada, C. Caloz, and T. Itoh, "Novel zeroth order resonance incomposite left/right handed transmission line resonators," in *Proceedings of the Asia-Pacific Microwave Conference*, pp. 1588–1591, Seoul, Korea, November 2003.

[7] R. W. Ziolkowski and A. Erentok, "Metamaterial-based efficient electrically small antennas," *IEEE Transactions on Antennas and Propagation*, vol. 54, no. 7, pp. 2113–2130, 2006.

[8] S. K. Sharma, A. Gupta, and R. K. Chaudhary, "Epsilon negative CPW-fed zeroth-order resonating antenna with backed ground plane for extended bandwidth and miniaturization," *IEEE Transactions on Antennas and Propagation*, vol. 63, no. 11, pp. 5197–5203, 2015.

[9] C. Caloz and T. Itoh, *Electromagnetic Metamaterials: Transmission Line Approach and Microwave Applications*, Wiley, Hoboken, NJ, USA, 2005.

[10] B. D. Bala, M. K. A. Rahim, and N. A. Murad, "Composite right/left-handed dual-band metamaterial antenna with improved gain and efficiency," *Microwave and Optical Technology Letters*, vol. 56, no. 7, pp. 1575–1579, 2014.

[11] A. Lai, K. M. K. H. Leong, and T. Itoh, "Infinite wavelength resonant antennas with monopolar radiation pattern based on periodic structures," *IEEE Transactions on Antennas and Propagation*, vol. 55, no. 3, pp. 868–876, 2007.

[12] T. Jang, J. Choi, and S. Lim, "Compact Coplanar Waveguide (CPW)-Fed Zeroth-Order Resonant antennas with extended bandwidth and high efficiency on vialess single layer," *IEEE Transactions on Antennas and Propagation*, vol. 59, no. 2, pp. 363–372, 2011.

[13] P.-L. Chi and Y.-S. Shih, "Compact and bandwidth-enhanced Zeroth order resonant antenna," *IEEE Antennas and Wireless Propagation Letters*, vol. 14, pp. 285–288, 2015.

[14] A. Gupta and R. Kumar Chaudhary, "A compact short-ended zor antenna with gain enhancement using ebg loading," *Microwave and Optical Technology Letters*, vol. 58, no. 5, pp. 1194–1197, 2016.

[15] A. Mehdipour, T. A. Denidni, and A. R. Sebak, "Multi-band miniaturized antenna loaded by ZOR and CSRR metamaterial structures with monopolar radiation pattern," *IEEE Transactions on Antennas and Propagation*, vol. 62, no. 2, pp. 555–562, 2014.

[16] R. Samson Daniel, R. Pandeeswari, and S. Raghavan, "A compact metamaterial loaded monopole antenna with offset-fed microstrip line for wireless applications," *AEU - International Journal of Electronics and Communications*, vol. 83, pp. 88–94, 2018.

[17] T. Ali, A. Mohammad Saadh, R. C. Biradar, J. Anguera, and A. Andújar, "A miniaturized metamaterial slot antenna for wireless applications," *AEU - International Journal of Electronics and Communications*, vol. 82, pp. 368–382, 2017.

[18] L.-M. Si, W. Zhu, and H.-J. Sun, "A compact planar and CPW-fed metamaterial-inspired dual-band antenna," *IEEE Antennas and Wireless Propagation Letters*, vol. 12, pp. 305–308, 2013.

[19] B. Zong, G. Wang, C. Zhou, and Y. Wang, "Compact low-profile dual-band patch antenna using novel TL-MTM structures," *IEEE Antennas and Wireless Propagation Letters*, vol. 14, pp. 567–570, 2015.

[20] B. P. Smyth, S. Barth, and A. K. Iyer, "Dual-band microstrip patch antenna using integrated uniplanar metamaterial-based

EBGs," *IEEE Transactions on Antennas and Propagation*, vol. 64, no. 12, pp. 5046–5053, 2016.

[21] S. K. Sharma, M. A. Abdalla, and R. K. Chaudhary, "An electrically small SICRR metamaterial-inspired dual-band antenna for WLAN and WiMAX applications," *Microwave and Optical Technology Letters*, vol. 59, no. 3, pp. 573–578, 2017.

[22] R. Kumar, R. Singh, and R. K. Chaudhary, "Miniaturised triple-band antenna loaded with complementary concentric closed ring resonators with asymmetric coplanar waveguide-fed based on epsilon negative transmission line," *IET Microwaves, Antennas & Propagation*, vol. 12, no. 13, pp. 2073–2079, 2018.

[23] C. J. Brochu, G. A. Morin, and J. W. Moffat, "Gain measurement of a cavity-backed spiral antenna from 4 to 18 GHz using the three-antenna method," *Defence Research Establishment Ottawa (ONTARIO)*, ADA359308, 1998.

[24] R. Jie, H. Jing, S. Li, and Y. Xiao, "Dual-band circular polarizers based on a planar chiral metamaterial structure," *IEEE Antennas and Wireless Propagation Letters*, vol. 18, no. 12, pp. 2587–2591, 2019.

[25] W. Kamonsin, P. Krachodnok, P. Chomtong, and P. Akkaraekthalin, "Dual-band metamaterial based on jerusalem cross structure with interdigital technique for LTE and WLAN systems," *IEEE Access*, vol. 8, pp. 21565–21572, 2020.

[26] M. Zada, I. A. Shah, and H. Yoo, "Metamaterial-Loaded compact high-gain dual-band circularly polarized implantable antenna system for multiple biomedical applications," *IEEE Transactions on Antennas and Propagation*, vol. 68, no. 2, pp. 1140–1144, 2020.

[27] X. Wu, X. Wen, J. Yang, S. Yang, and J. Xu, "Metamaterial structure based dual-band antenna for WLAN," *IEEE Photonics Journal*, vol. 14, no. 2, pp. 1–5, Article ID 7722105, 2022.